Received January 17, 2020, accepted February 15, 2020, date of publication February 27, 2020, date of current version March 13, 2020.

Digital Object Identifier 10.1109/ACCESS.2020.2976643

Analysis and Design of Reflectarray Antennas Based on Delay Lines: A Filter Perspective

JIAWEI ZANG[1], (Member, IEEE), EDUARDO CARRASCO[2], (Senior Member, IEEE), XUETIAN WANG[3], ALEJANDRO ALVAREZ-MELCON[4], (Senior Member, IEEE), AND JUAN SEBASTIAN GOMEZ-DIAZ[5], (Senior Member, IEEE)

[1]China Academy of Information and Communications Technology, Beijing 100191, China
[2]Information Processing and Telecommunication Center, Universidad Politécnica de Madrid, 28040 Madrid, Spain
[3]School of Information and Electronics, Beijing Institute of Technology, Beijing 100081, China
[4]Departmento de Tecnologías de la Información y las Comunicaciones, Universidad Politécnica de Cartagena, 30202 Cartagena, Spain
[5]Department of Electrical and Computer Engineering, University of California at Davis, Davis, CA 95616, USA

Corresponding author: Alejandro Alvarez-Melcon (alejandro.alvarez@upct.es)

This work was supported by the National Science Foundation with a CAREER Grant No. ECCS-1749177 by the Technical University of Madrid through the Programa Propio de I+D+i under Grant ECCS-1749177, and in part by the Spanish Government under Project TEC2016-75103-C2-1-R and Project TEC2016-75934-C4-4-R. The work of Jiawei Zang was supported by the China Scholarship Council under Grant 201706030132. The work of Alejandro Alvarez-Melcon was supported by the Spanish Government under Grant 20147/EE/17 and Grant PRX18/0009256.

ABSTRACT The analysis and design of reflectarray (RA) antennas based in delay lines is introduced for the first time from a filter perspective. To this purpose, each unit-cell of the RA is considered as a network composed of two ports, one being the delay line and the other one the free-space. This approach allows to borrow the coupling matrix formalism from filter theory and apply it to design unit-cells exhibiting broadband operation together with very sharp frequency responses. The concept is demonstrated with the aid of planar printed unit-cells coupled to substrate integrated waveguides (SIWs) through slots, a configuration that offers significant advantages to shape its frequency response while providing relatively low loss. With the aim of validation, a third order filter structure integrated in SIW-based unit-cells has been experimentally tested using the waveguide simulator technique, at a center frequency of 9 GHz. Measurements demonstrate a high-quality linear phase variation and range, and large frequency selectivity together with broadband response for the element of about 18%. The experimental results show the feasibility of this approach for the design of broadband reflectarray antennas exhibiting sharp gain responses. To illustrate the concept, a medium size reflectarray has been theoretically designed using the proposed unit cell at 9 GHz, showing a directive beam with 35.8 dB gain, sharp gain selectivity over 18 dB, and confirms the wide band operation with 20.3% bandwidth for a 3 dB gain variation.

INDEX TERMS Broadband antennas, delay-line elements, filter theory, gain selectivity, reflectarray antennas, substrate integrated waveguide.

I. INTRODUCTION

Reflectarray (RA) antennas have gathered together the benefits of parabolic reflectors and phase array antennas into low-cost, planar, and efficient structures [1]. Modern RA configurations find exciting applications in terrestrial/satellite communication and radar systems [2]–[4]. The analysis and design of RA antennas usually requires to (i) determine the phase-shift and electromagnetic response of the composing unit-cells versus some geometrical/material parameter variation, rigorously considering mutual coupling effects and the influence of the incident angle of the incoming wave to each cell; (ii) gather together slightly different cells to engineer a specific surface phase-profile that implements a desired RA performance; and (iii) evaluate the radiation properties of the entire structure considering the different phase delay between the feeder and the cells. The development of advanced unit-cells exhibiting large phase-shift ranges and intriguing responses –for instance, in terms of polarization [5], multifrequency operation [6], reconfigurability [7], using advanced elements rotation techniques [8], or by integrating SIW antennas as feeders [9]– has undoubtedly driven RAs technology in the last years.

The associate editor coordinating the review of this manuscript and approving it for publication was Qingfeng Zhang.

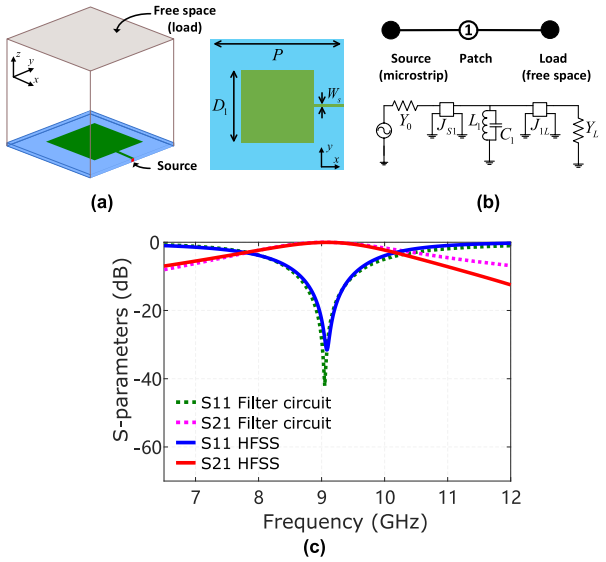

FIGURE 1. True-time delay unit-cell based on a patch antenna with an attached stub printed over a grounded dielectric. (a) Geometry of the cell. (b) Cell coupling topology (top) and its equivalent circuit (bottom). (c) Filter circuit and simulated scattering parameters in amplitude for the cell. The size of the square unit-cell is $P = 16.7$ mm, the patch width is $D_1 = 9.72$ mm, and the stub width is $W_S = 0.3$ mm. The dielectric has a thickness, permittivity, and loss tangent of $h = 1.57$ mm, $\epsilon_r = 2.2$, and $tan\delta = 0.0009$, respectively.

The most severe drawback of RA antennas is arguably their narrow operational bandwidth, which is determined by the resonant response of their composing unit-cells and the different phase delay between such cells and the feeder [1]. Recent years have rapidly seen a growing interest to enhance this bandwidth, mainly through RA antennas composed of unit-cells that provide various resonant frequencies [10]–[14] or that exhibit a true-time delay (TTD) response [15]–[20]. For multi-resonant elements, the dimensions of the resonators that compose the unit-cells are modified to resonate at slightly different frequencies, which provides the required 360° phase-shift. On the other hand, TTD elements are more attractive, since large phase variations can be easily achieved only by adjusting the length of delay lines with no need to change elements size.

For instance, a classical approach for the design of a TTD reflectarray unit cell uses a simple patch antenna coupled to a microstrip line, as shown in Fig. 1(a) [21]–[23]. The TTD operation is achieved with the adjustment of the microstrip line length, to introduce the required phase shift to the signal. From a circuital point of view, the operation of the patch can be modeled as a single resonator coupled to the microstrip line on the input port, and to the free space on the output port, as sketched in Fig. 1(b). A limitation of this configuration is the small rejection provided by the unit cell as can clearly be observed in Fig. 1(c). While this behavior leads to wide band operation [see Fig. 1 (c)], the main consequence of this small rejection is that the gain of RA antennas usually exhibits a smooth response versus frequency [18], [24]. As a result, these antennas cannot be applied in communication systems based on frequency-selectively channels or in sensitive defense/military applications.

In the above context, this contribution proposes for the first time to analyze and design reflectarray unit-cells from a filter perspective, with the purpose to increase selectivity and rejection to adjacent channels. Using the coupling matrix approach [25], [26], the design of complex filtering transfer functions between the delay line and the free-space can be efficiently accomplished, allowing the implementation and manipulation of transmission zeros to achieve high selective responses. Inspired by these concepts, we propose to merge filter theory and reflectarray elements based in delay lines to provide new perspective and physical insight to realize RA antennas. The implementation of such transmission zeros would result, for the first time, on RA antennas exhibiting very sharp gain responses with frequency. Even though this approach is based on using resonant elements, relatively large bandwidths can still be obtained. This can in fact be achieved by increasing the couplings between the resonators in the filter structure, including the input and output couplings.

To implement this concept, we propose to employ a compact unit-cell using SIW technology. The cell is composed of a resonant patch and several resonant slots, coupled to a SIW-based structure [15], [16]. The resonant elements conform the filtering to free space, while the SIW structure introduces the flexibility in the achievable phase shift, in which the phase is controlled by adjusting the length of a delay line [16]–[19]. Preliminary designs of this unit-cell concept were proposed by some of the authors in [16]. This cell is planar, easy to manufacture, low-loss compared to microstrip technology as frequency increases, and it provides additional advantages as compared to standard microstrip delay lines, including TTDs cells [17]. They require one less dielectric layer in the multi-stack and avoid undesirable back radiation. In this paper we use this unit-cell as a platform to demonstrate how advanced filtering configurations can be implemented in reflectarray antennas, and such unit-cells can be engineered to enhance its bandwidth and to introduce and control transmission zeros for maximum selectivity.

Even though the multilayered unit-cells proposed here might be more challenging to implement than common single-layer cells [10], they lead to reflectarrays exhibiting far superior performance. Specifically, the proposed cells permit to easily integrate several coupled resonances to significantly enhance the antenna bandwidth and provide highly-selective frequency responses while keeping excellent efficiency. Once the resonances and couplings are optimized, large phase variations can be easily achieved only by adjusting the length of the SIW. In addition, the proposed cell reduces back radiation and losses as frequency increases, as compared to microstrip technology [22], [23]. It also keeps the possibility to easily integrate electronic circuits, with the advantage of having the control circuits in the back side of the antenna, therefore separated from the radiation side.

In order to demonstrate the practical feasibility of the concept, several unit cells with increasing SIW lengths have

been manufactured and tested using the waveguide simulator technique [19]–[27]. Measurements monitor the phase shift introduced by the unit cell as a function of the SIW lengths, for different frequencies inside and outside the useful bandwidth. Results confirm a high-quality linear phase shift dependence with the SIW length for frequencies inside the passband, while it shows no responsiveness for frequencies outside the passband. This exciting behavior demonstrates the potential of the new proposed concept for the design of broadband reflectarrays with sharp gain response.

II. UNIT –CELLS BASED IN DELAY LINES: A FILTER PERSPECTIVE

Fig. 1(a) represents the traditional unit cell used in the design of RA antennas using delay lines [1]. As already explained, a resonant patch couples on one side to the free space allowing radiation, and on the other end to a standard microstrip line. The microstrip line is used to provide a phase shift proportional to its length. The simulation of all unit cells in this paper always uses periodic boundary conditions to account for the coupling between adjacent elements in a periodic environment, usually done in RA analysis [1]. In addition, the free space port is modeled as a Floquet port, selecting the fundamental harmonic. From a circuital perspective, the structure shown in Fig.1(a) is known as an in-line filter as sketched in Fig. 1(b) [28]. This coupling topology does not contain cross couplings between non-adjacent elements, and thus transmission zeros cannot be implemented in the response. Using the coupling matrix formalism [25], the normalized coupling matrix of this structure is simply

$$M_1 = \begin{bmatrix} 0 & 1.38 & 0 \\ 1.38 & 0 & 1.38 \\ 0 & 1.38 & 0 \end{bmatrix} \quad (1)$$

The large normalized coupling value shown in Eq. (1) allows to obtain wide bandwidths, but at the expense of reduced rejection levels, as indicated in the response of Fig. 1(c). In this figure, the electromagnetic response obtained with the commercial software HFSS [29] is compared with the response obtained from the equivalent circuit also shown in Fig. 1(b). It can be observed good agreement between the two responses close to the resonance. Far from the resonance the two responses start to diverge, due to dispersive effects of the patch antenna that are not present in the simple lumped based equivalent circuit.

With the aim of increasing the rejection levels without reducing the bandwidth, we now propose alternative delay-line RA cells, which integrate a filter unit with a SIW based transmission line, as shown in Fig. 2. In Fig. 3 we detail the frequency responses of the new proposed cells [Fig. 3(b)-(d)], together with the response of the original simple patch antenna cell, already discussed [Fig. 3(a)]. Fig. 2(a) shows a second order filter integrated with the SIW line, composed of a resonant patch and a resonant slot. Since the SIW line is a closed structure, the input SIW port only couples to the slot [resonator 1 in Fig. 2(a)]. However, the slot is able to radiate to free space, and also by proximity to have some electromagnetic coupling to the patch. Of course, the patch itself can radiate to free space, given rise to the coupling

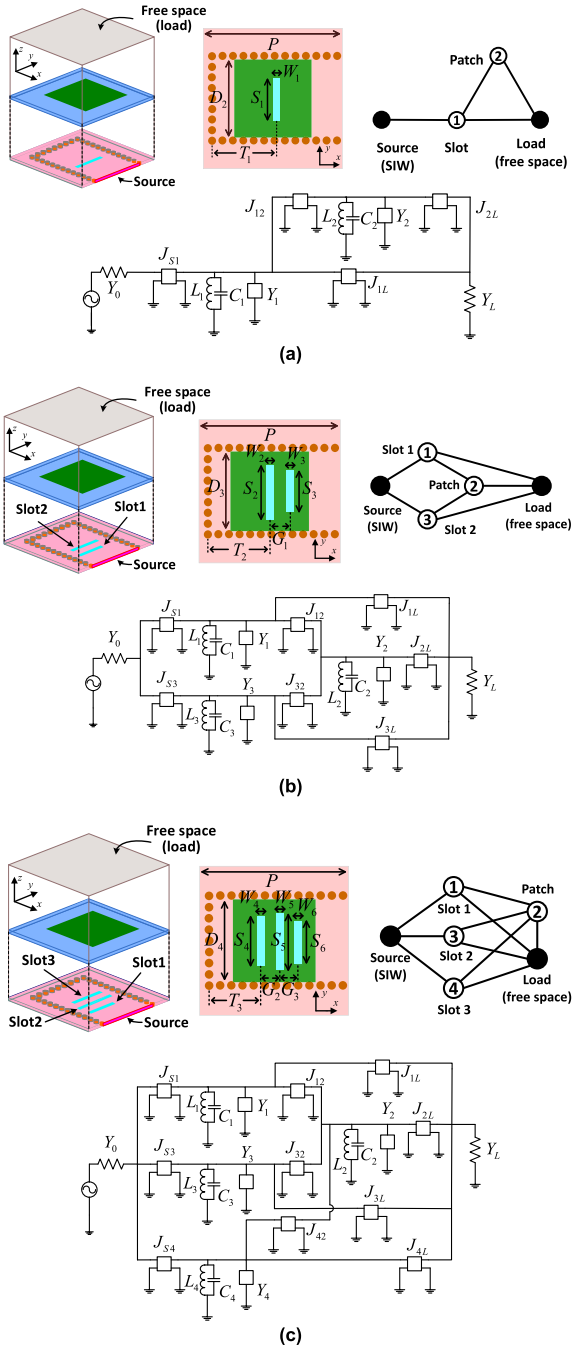

FIGURE 2. Unit-cells based on a patch antenna coupled to a SIW delay line through one (a), two (b) and three (c) slots. For each case, left and central panels show the 3D and top views, respectively. The right and bottom panels illustrate the cell coupling topology and its equivalent circuit. The size of the unit-cell and the features of the top dielectric are similar to the ones described in Fig. 1. The multi-stack structure is shown in parts for illustration, but after assembling there is no any air gap between the SIW and the patch substrates. The dielectric of the SIW line has a thickness, permittivity, and tangent loss of $h = 0.38$ mm, $\epsilon_r = 6$, and $tan\delta = 0.0023$, respectively. Other parameters are $D_2 = 9.52$ mm, $D_3 = 9.53$ mm, $D_4 = 9.35$ mm, $S_1 = 5.2$ mm, $S_2 = 5.8$ mm, $S_3 = 5$ mm, $S_4 = 5.5$ mm, $S_5 = 6.4$ mm, $S_6 = 48$ mm, $W_1 = 0.8$ mm, $W_2 = W_3 = 0.8$ mm, $W_4 = W_5 = W_6 = 0.85$ mm, $G_1 = 2.4$ mm, $G_2 = 2.1$ mm, $G_3 = 2$ mm, $T_1 = 7.8$ mm, $T_2 = 7.6$ mm, and $T_3 = 5.9$ mm.

topology shown in Fig. 2(a) (top-right). It can be observed that this coupling topology does not follow anymore the traditional in-line configuration. In fact, a cross coupling from the slot and free space occurs, leading to a so called tri-section topology [30]. This topology admits the implementation of one transmission zero at finite frequencies as shown in the response of Fig. 3(b). The coupling matrix for this response clearly shows the properties described above, and it leads to

$$M_2 = \begin{bmatrix} 0 & -1.201 & 0 & 0 \\ -1.201 & -0.585 & 1.309 & -0.542 \\ 0 & 1.309 & 0.739 & 1.072 \\ 0 & -0.542 & 1.072 & 0 \end{bmatrix} \quad (2)$$

It can be observed that the topology becomes asynchronous, so that slot and patch are tuned at slightly different resonant frequencies. The shift in resonant frequency is in fact given by the non-zero elements in the diagonal of the coupling matrix [25], [26]. Also, the position of the transmission zero below the passband is due to the negative sign of the couplings observed in Eq. (2). These negative signs are possible due to the different coupling mechanisms, electric or magnetic, involved in the couplings to the slot and patch elements. In Fig. 3(b) the response of the coupling matrix is also included, and it is compared with full wave simulations obtained with HFSS. Again, the agreement between the two responses is remarkable.

Following a similar strategy, the order of the filter integrated in the SIW line can be increased by introducing additional resonant slots along the SIW top cover. The concept is illustrated in Fig. 2(b) where a second resonant slot is incorporated to the structure. Again, because the SIW is a closed waveguide, the SIW port can only couple to the two slots. However, both slots can couple to the patch and to free space. Then, it is easy to verify that the coupling topology of the resulting filter is the one shown in the sketch (top-right) of Fig. 2(b). The coupling topology indicates that more cross couplings are introduced by this structure, allowing to produce two transmission zeros at finite frequencies, as indicated by the response shown in Fig. 3(c). The coupling matrix of the discussed topology, this time becomes

$$M_3 = \begin{bmatrix} 0 & 0.953 & 0 & 0.01 & 0 \\ 0.953 & 0.002 & 0.73 & 0 & -0.299 \\ 0 & 0.73 & -0.187 & 0.979 & -0.145 \\ 0.01 & 0 & 0.979 & 0.246 & 0.893 \\ 0 & -0.299 & -0.145 & 0.893 & 0 \end{bmatrix} \quad (3)$$

In general, the implementation of the filter response using the structure shown in Fig. 2(b) may be challenging. This is because the coupling from the SIW port to the slot mainly depends on the distance to the back short circuit (T_2). Since the two slots should be placed at different positions, then only one of the slots can have strong coupling to the SIW port. Fortunately, the coupling matrix shown in Eq. (3) indicates that the SIW port only needs strong coupling to the first slot (resonator 1, $M_{S1} = 0.953$) while the coupling to the second slot (resonator 3) can be very small ($M_{S3} = 0.01$). This

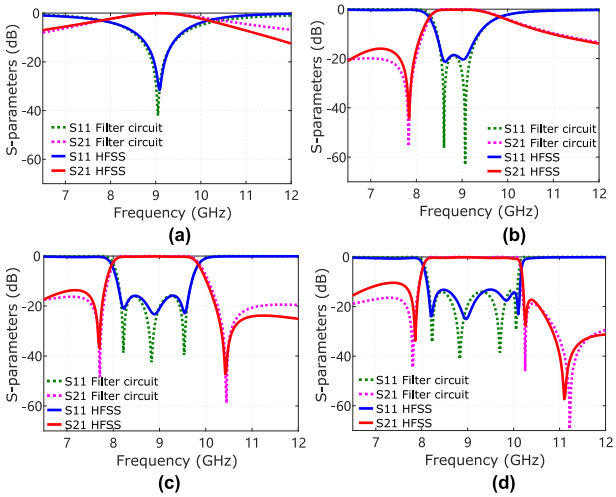

FIGURE 3. Scattering parameters of true-time-delay unit-cells located in a periodic environment and excited through their phase-delay lines. Results are computed using circuit theory and have been validated with full-wave simulations. Panels (a), (b), (c), and (d) corresponds to the cells described in Fig. 1 and Figs. 2a, 2b, and 2c, respectively.

property also suggests that more slots can be added to the structure to conceive higher order filters, as it will be shown next. Fig. 3(c) shows the response of the derived coupling matrix, together with full wave results of the unit cell obtained with HFSS. Again, the agreement is very good, especially close to the passband.

As suggested in the previous paragraph, the same strategy can be followed to obtain a filter structure of fourth order, just by incorporating an additional slot on the top plate of the SIW line [see Fig. 2(c)]. Similar concepts as introduced before, lead to the coupling topology also shown in Fig. 2(c) (top-right). This topology implements three transmission zeros at finite frequencies, one below the passband and two above the passband, as indicated by the response shown in Fig. 3(d). Again, the position of the slots with respect to the back short circuit indicate that the SIW port can only have strong coupling to one of the slots. Fortunately, the coupling matrix of the transfer function again indicates that small couplings are needed between the SIW port and the second and third slots [resonators 3 and 4 in Fig.2 (c) (top-right)]. This can be observed in the (M_{S3}) and (M_{S4}) elements of the coupling matrix representing the corresponding transfer function, which is

$$M_4 = \begin{bmatrix} 0 & 0.877 & 0 & 0.01 & 0.002 & 0 \\ 0.877 & 0.043 & 0.722 & 0 & 0 & -0.186 \\ 0 & 0.722 & -0.194 & 0.574 & -0.103 & -0.308 \\ 0.01 & 0 & 0.574 & 0.757 & 0 & 0.687 \\ 0.002 & 0 & -0.103 & 0 & -1.038 & 0.409 \\ 0 & -0.186 & -0.308 & 0.687 & 0.409 & 0 \end{bmatrix} \quad (4)$$

Fig. 3(d) compares the responses of both full wave simulations obtained with HFSS and the response of the coupling matrix given in Eq. (4), obtaining good agreement.

The element values of the equivalent circuits shown in Fig. 2 -for all the designed cells- can be obtained from the calculated coupling matrices by simply applying standard scaling techniques. From the lowpass prototype with all elements normalized to one, represented by the coupling matrix, the application of the standard lowpass to bandpass transformation [28] leads to the following LC resonator

$$C_i = \frac{1}{2\pi f_{BW}}; \quad i = 1, 2, 3, 4 \tag{5}$$

$$L_i = \frac{1}{(2\pi f_o)^2 C_i}; \quad i = 1, 2, 3, 4 \tag{6}$$

where f_{BW} is the bandwidth, and f_0 is the center frequency of the passband response. Note that in this representation all resonators are equal ($C_4 = C_3 = C_2 = C_1, L_4 = L_3 = L_2 = L_1$). The constant susceptances (Y_i) shown in Fig. 2 are used to take into account for displacements in the resonant frequencies of the different resonators in asynchronously tuned topologies. These are directly translated from the diagonal elements of the coupling matrix as

$$Y_i = jM_{ii}; \quad i = 1, 2, 3, 4 \tag{7}$$

For inter-resonator couplings, the off-diagonal elements of the coupling matrix directly give the values of the corresponding admittance inverters of the circuit (J_{mn}) namely

$$J_{mn} = M_{mn}; m \text{ and } n = 1, 2, 3, 4 \tag{8}$$

For the input and output couplings, however, some care must be taken, since the SIW line and the free space ports exhibit different characteristic admittances (Y_0 and Y_L respectively). In fact, full wave calculations lead to a value of $Y_0 = 1/10$S for the SIW ports, while the standard admittance value $Y_L = 1/(120\pi)$S needs to be taken for free space ports. This difference in the port admittances is absorbed in the first and last admittance inverters with a proper scaling of the corresponding elements of the coupling matrix, as

$$J_{st} = M_{St}\sqrt{Y_0} \tag{9}$$

$$J_{pL} = M_{pL}\sqrt{Y_L} \tag{10}$$

It should be noted that the responses given in Fig. 3 have been obtained from the analysis of the equivalent circuits shown in Fig. 2, with the element values calculated according to (5)-(10).

Note that the coupling matrices given in this section (2)-(4), can also be used to assist in the design of the physical structures shown in Fig. 2. The lengths of the slots (S_i) and of the patch (D_i) determine the resonant frequencies of the resonators (f_{ri}). These can directly be obtained from the diagonal elements of the given coupling matrices (M_{ii}) using the relation

$$f_{ri} = \frac{1}{2} f_{BW} \left[-M_{ii} + \sqrt{M_{ii}^2 + \frac{4f_0^2}{f_{BW}^2}} \right] \tag{11}$$

Once the resonant frequencies of the resonators are adjusted, the next step is to adjust the couplings between the different elements of the structure given by the off-diagonal terms of the coupling matrices. The couplings between the input SIW and the output free space ports (M_{St}, M_{pL}) can be adjusted by controlling the positions of the slots and the patch (T_i) and (G_i). In general, this can be done through the external quality factors of singly terminated resonators [25]–[28], calculated as

$$(Q_{ext})_{IN} = \frac{f_0}{M_{St}^2 f_{BW}} \quad (Q_{ext})_{OUT} = \frac{f_0}{M_{pL}^2 f_{BW}} \tag{12}$$

Finally, the couplings between the slots and the patch (M_{mn}) can be adjusted with the relative position of the patch with respect to the slots (G_i). This can be done with the adjustment of the inter-resonator couplings between two internal resonators [25]–[28], calculated as

$$k_{mn} = M_{mn} \frac{f_{BW}}{f_0} \tag{13}$$

It is important to remark that since the diagonal elements of the coupling matrices are different from zero, the general procedure described in [31] for asynchronously tuned topologies must be applied when extracting these coupling factors. After all the elements are dimensioned separately as described, they are assembled together into the final structure. Due to electromagnetic interactions between all the elements and loading effects of couplings into resonators [25], a final optimization of the global structure is needed to obtain the final dimensions collected in the caption of Fig. 2.

Note that with the strategy proposed, that consists on increasing the order of the filter, the bandwidth of the unit-cell cannot be increased much further. This is because the bandwidth is determined primarily on the amount of coupling from the ports to the different resonant elements of the structure, and this is similar in the three configurations shown in Fig. 2. In fact, the bandwidths measured at constant return loss of 13 dB for the four designs presented are 6.5%, 8.9%, 17.3%, and 21.9%. The filter approach allows to improve the bandwidth of the reflectarray cell in a simple way, reducing the design of the phase-shifter to optimizing the length of the delay-line, as in the case of TTD RA [17]. In addition, the big benefit of the strategy proposed is that the selectivity and rejection between adjacent channels is largely improved, especially due to the possibility to implement and to control transmission zeros in the responses of the RA cells. This in turn leads to sharp variations in the gain of the antenna, as it will be shown later in this paper.

As a last remark, note that although the concept of integrating a filter unit in the structure of an RA cell, and the possibility to introduce and control transmission zeros has been illustrated with a host unit cell implemented in SIW technology, these concepts are general, and could be applied to RA cells conceived in other technologies.

III. UNIT CELL VALIDATION

The reflection phase responses of the three slots unit cell [see Fig. 2(c)] as a function of the SIW length are shown

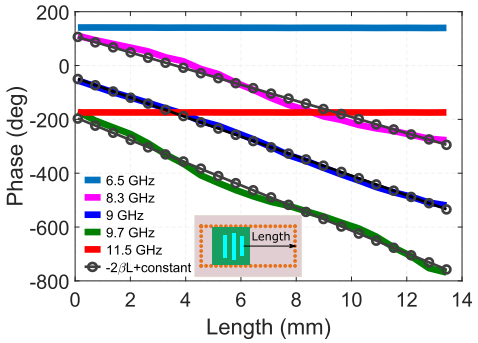

FIGURE 4. Reflection phase at the surface of the unit-cell shown in Fig. 2(c) as a function of SIW length. The cell, excited from free space, has been short-circuited at the end of the SIW (see inset). Results, plotted for different frequencies, are computed using full-wave simulations (solid) and using the theoretical SIW propagation constant (dotted). Other parameters are as in Fig. 2.

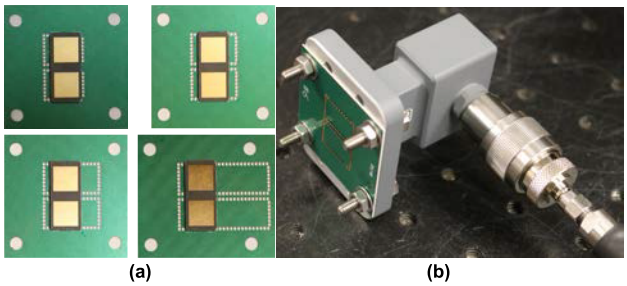

FIGURE 5. Experimental set-up to validate the proposed SIW-based RA unit-cell. (a) Manufactured cells with four different lengths for the SIW line. (b) One cell mounted in a WR90 waveguide section.

in Fig. 4 for different frequencies including frequencies inside and outside the unit-cell bandwidth. Within the passband, the phase responses show a very linear dependence versus frequency. These characteristics are excellent, since they indicate that the incoming power is effectively coupled to the SIW phase-delay line and then it propagates in the forward and backward directions along the line, obtaining the required phase shift. It is also observed that the behavior of the phase for these frequencies is close to the situation of an ideal delay line. For the SIW line the propagation constant is calculated to be 261.7, 316.8, and 367.2 rad/m at 8.3, 9, and 9.7 GHz, respectively.

In Fig. 4 we can compare the phase of the unit cells calculated with full wave simulations (HFSS) (solid lines) with the analytical calculations based on the theoretical propagation constant model (circle symbols). It can be observed good agreement between full wave and theoretical results, thus demonstrating the operation as a simple delay line. Moreover, for out-of-band frequencies, the reflecting phases are almost constant as the SIW length increases. This behavior clearly indicates that the incoming power cannot couple to the SIW line of the unit-cell, and therefore the reflected waves always exhibit a similar phase, independently on the SIW length. These unique phase responses are helpful for obtaining wideband and high gain selectivity performance, as it will be shown in the next section.

To demonstrate the practical feasibility of the idea proposed in this paper, the element shown in Fig. 2(b) (two slots) has been experimentally validated by using the well-known waveguide simulator technique [27]. Here, the SIW is fabricated using a Rogers Corporation RO4360G2 laminate with a thickness of 0.406 mm, a relative permittivity of 6.15, and a loss tangent of 0.0038. The fabrication of the unit cells in SIW technology does not represent nowadays a major challenge, as a similar PCB technology as used in the electronics circuit industry can be employed to manufacture SIW circuits. This also applies to the more specific implementation of metalized via-holes needed by SIW technology. In Fig. 5 we include a photo of the manufactured prototypes, showing the additional integration of the patch substrate on top of the SIW structure. All prototypes have been manufactured by Bay Area Circuits [32], using a tolerance in all PCB processes of 70 μm.

To design the waveguide simulator two unit-cells were inserted into a WR-90 waveguide section, and the reflection coefficient was measured with a Vector Network Analyzer (VNA) for different lengths of the SIW. The experimental setup and the manufactured unit cells for four different SIW lengths are shown in Fig. 5. Measured results for the phase and magnitude of the reflection coefficient for 15 different SIW lengths are shown in Fig. 6. Fig. 6(a) includes measurements of the phase at four different frequencies inside the passband (8.4, 9, 9.5, and 10 GHz) of the cell. Solid lines indicate full wave simulations obtained with HFSS, while symbols denote measured results. We can observe good agreement between them, thus confirming the practical feasibility of the proposed structure. Fig. 6(b) shows the phase response at band-edge and out-of-band frequencies. Again, the agreement between measured and simulated results is very good. This test experimentally confirms that the responsiveness of the phase with the SIW length abruptly changes around the edge of the passband (see inset of panel (a)). Finally, Fig. 6(c) shows the magnitude of the reflection coefficient, related to losses, for two frequencies. The first one is the center frequency inside the passband (9 GHz), and the second one is located out of the passband (11 GHz). When the frequency is outside the passband, the losses are almost constant with the SIW length, indicating that the power is not coupled and therefore it is not dissipated inside the SIW line. On the contrary, when the frequency lies inside the passband, some power is dissipated inside the SIW line, so the losses increase with its length, as also happens with delay lines realized with microstrip technology [17]. In this last case, some of the manufactured unit cells exhibit slightly higher losses than expected. We attribute this loss increase to the poor contact between the waveguide flange and the SIW ground plane, to potential misalignments between the slots and the waveguide, and to the small gap that might be created between the substrates. Some of these loss mechanisms will not appear in the entire reflectarray because the bonding

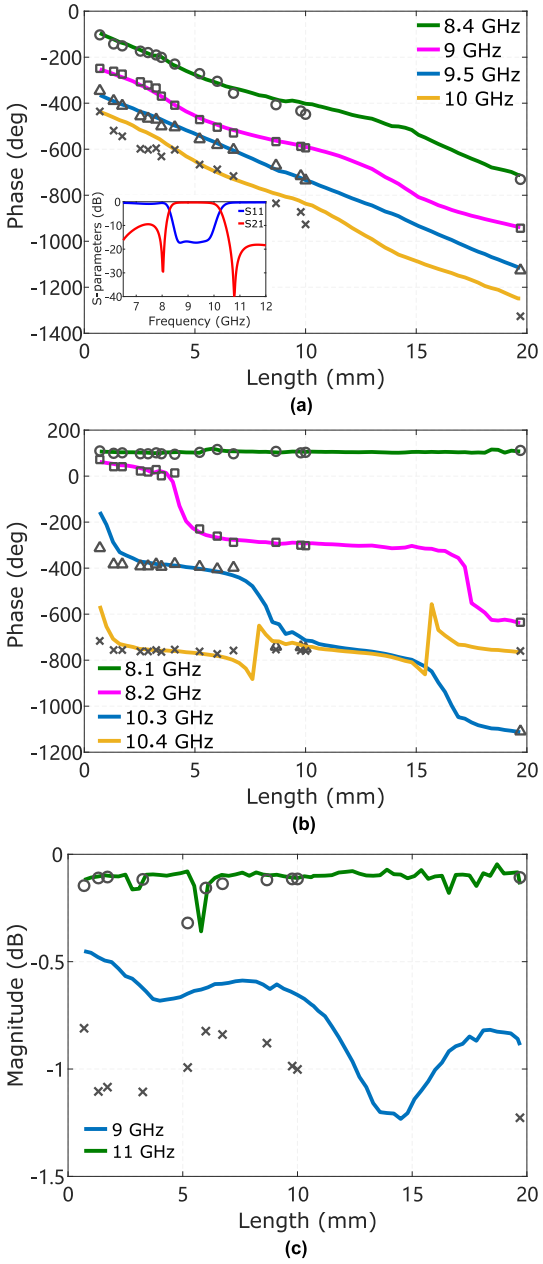

FIGURE 6. Electromagnetic response of the fabricated unit-cells using the waveguide simulator technique [19], [27]. Measured (markers) and simulated data (solid lines) are plotted versus the length of the SIW line, i.e., each point correspond to a different unit-cell. The reflection phase is shown in the pass-band (a) and in the band-edge/out-of-band (b) of cells. Inset in panel (a) shows simulated S parameters of the cells. (c) Magnitude of reflection coefficient (S_{11}).

process will ensure a good contact between the layers, and the waveguide flange is only present in this measurement technique, not in a real reflectarray. In any case, average losses are expected to be around 0.7 dB.

IV. DESIGN GUIDELINES FOR A COMPLETE REFLECTARRAY

An offset circular RA composed of 50 × 50 unit cells using the three slots elements [see Fig. 2(c)] with a main beam in the direction $\theta_0 = 18°$ and $\varphi_0 = 0°$ has been

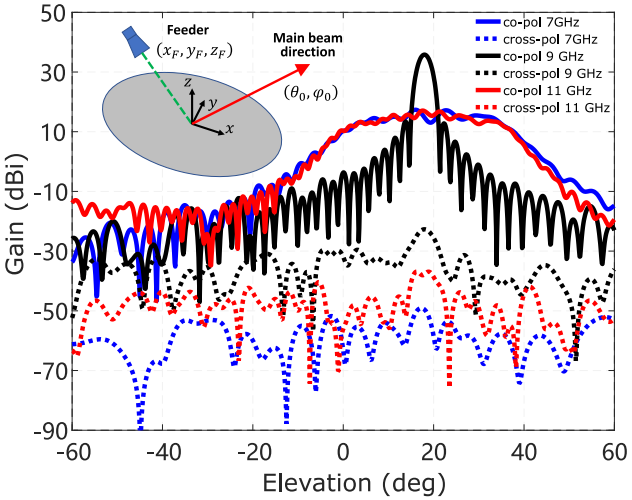

FIGURE 7. Radiation patterns of a reflectarray composed of 50 × 50 unit-cells as the one described in Fig. 2c for various operation frequencies and polarizations. The reflectarray is designed to point towards $\theta_0 = 18°$ and $\phi_0 = 0°$. An x-polarized horn antenna, located at $(x_F, y_F, z_F) = (-322, 0, 838)$ mm with respect to the reflectarray center and modelled with a $\cos^q(\theta)$ function with $q = 10$, is employed to illuminate the antenna. Other parameters are as in Fig. 2.

designed, using the phase information given in Fig. 4. The radiation patterns in the elevation plane are given in Fig. 7. The x-polarized feed horn is modeled by a $\cos^q(\theta)$ function with $q = 10$ and located at the position $x_F = -322$ mm, $y_F = 0$, and $Z_F = 838$ mm, with respect to the RA center (see inset of Fig. 7). A bent SIW unit cell configuration with periodicity of half the free-space wavelength at 9 GHz is employed, which can provide a full phase coverage with a compact size [15]. We should stress that with the use of this bent configuration [15], the element spacing needs not to be increased to obtain the full 360° variation in the phase of the reflection coefficient.

As can be seen from Fig. 7, when the frequency lies inside the passband of the element, the desired high directive beam is achieved. This is because the unit cells of the RA provide the required phase shift to compensate for the spatial phase delay between the feeder and the different elements of the RA. A maximum gain of 35.8 dB is obtained with a cross-polar level 54 dB below the maximum gain This scenario is quite different when the operation frequency lies out of the passband. In this case the signal cannot couple to the SIW line, so the reflection phase provided by each element is almost constant as already discussed. In this situation the radiating beam is not shaped, and the structure behaves as a metallic reflector with respect to the feeder, with a gain around 17.2 dB.

Fig. 8 shows the antenna gain as a function of frequency for four reflectarray antennas based on the discussed unit-cell elements. All RA antennas have the same configuration as shown in Fig. 7. The gain plot using a simple copper ground plane -with similar physical dimensions- has also been included, as a reference. Compared to the conventional

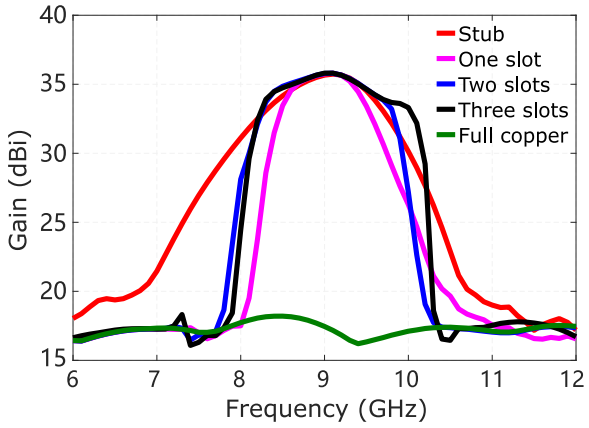

FIGURE 8. Maximum gain versus frequency of various reflectarray antennas designed as in Fig. 7. The reflectarrays are designed using the unit-cells described in Fig. 1 (red), and Figs. 2a (magenta), 2b (blue), and 2c (black). The response of a copper plane with the same dimensions as the reflectarray is included for comparison purposes. Other parameters are as in Fig. 2.

patch of Fig. 1, the new cells shown in Fig. 2 - with one, two and three slots - exhibit a very sharp gain selectivity of over 18 dB. This behavior can be attributed to the increasing order of the filter units integrated in the RA cells, and to the transmission zeros implemented at finite frequencies. These transmission zeros play a significant role in the abrupt frequency transitions observed in Fig. 8. The bandwidths for a 3-dB gain variation are 12.2%, 17.7%, and 20.3% for one slot, two slots, and three slots case, respectively. Note that the gain curves of these RA antennas in the out-of-band range are very similar to the simple ground plane case, which is due to the constant reflection phase they provide there (see Fig. 4). These plots clearly show that the introduction and manipulation of transmission zeros in the unit-cells can significantly improve the gain bandwidth and selectivity of RA antennas.

With respect to the behavior of the gain shown in Fig. 8, we have checked the radiation patterns of the designed array at the edge frequencies of the passband (8.3 GHz and 10 GHz). The beam-squint with frequency was minimized by properly selecting the position of the feeder [33]. The results obtained show almost no beam-squint with frequency (lower than 0.5°). In addition, radiation patterns at the extreme frequencies still exhibit good gain and low side lobe levels (SLL). We have checked that the SLL remains better than −20 dB within the frequency range from 8.45 GHz to 9.45 GHz. Then, it deteriorates towards the edges of the passband, although it remains better than −13.6 dB inside the whole bandwidth. This last test confirms the broadband operation of the designed reflectarray.

The proposed cell can potentially be used as a TTD, but its impact in the designed reflectarray is moderate due to the sharp frequency selectivity. Moreover, the broadband behavior of the unit cell allows to still achieve large bandwidth. To confirm this behavior, we have designed a similar reflectarray but applying phase truncation. Results show very similar performance in terms of the radiated patterns. For instance, the bandwidth was still of 20.3% for a 3-dB gain variation. In addition, the beam-squint in the same frequency range was lower than 0.8° for the phase truncated RA.

V. CONCLUSION

This paper has proposed novel delay-line reflectarray (RA) antennas from a filter design perspective. Considering the RA unit-cells as two-port network circuits, one coupled to the delay-line and the other one to free-space, has permitted to borrow the coupling matrix formalism from filter theory and apply it to gain great insight into the RA behavior, enabling new functionalities such an enhanced bandwidth and the implementation and precise control of transmission zeros to achieve a sharp frequency response. These exciting responses have been numerically and experimentally validated using a novel type of unit-cell composed of printed patches coupled to a SIW line through slots. One of these unit cells, operating at 9 GHz, has been manufactured and successfully tested using the waveguide simulator technique. Measured results confirm the broadband operation of the unit cell, exhibiting very linear phase variations with the SIW length in an 18% fractional bandwidth. A medium size reflectarray has been theoretically designed using this unit cell, showing a main beam with 35.8 dB gain, and very sharp gain selectivity of over 18 dB. Broadband operation has also been obtained with a fractional bandwidth of 20.3% for a 3-dB gain variation, with side lobe levels better than −20 dB. The proposed approach, which could be implemented in other technologies, will enable the development of broadband reflectarray antennas exhibiting sharp gain responses, with direct application in communication systems with frequency-selective channels or in the defense/military industry.

ACKNOWLEDGMENT

Alejandro Alvarez-Melcon was on leave at the Department of Electrical and Computer Engineering, University of California at Davis, Davis, CA 95616, USA.

REFERENCES

[1] J. Huang and J. A. Encinar, *Reflectarray Antennas*. Piscataway, NJ, USA: Wiley, 2007.
[2] Q. Luo, S. Gao, C. Zhang, D. Zhou, T. Chaloun, W. Menzel, V. Ziegler, and M. Sobhy, "Design and analysis of a reflectarray using slot antenna elements for Ka-band SatCom," *IEEE Trans. Antennas Propag.*, vol. 63, no. 4, pp. 1365–1374, Apr. 2015.
[3] W. Menzel, D. Pilz, and R. Leberer, "A 77-GHz FM/CW radar front-end with a low-profile low-loss printed antenna," *IEEE Trans. Microw. Theory Techn.*, vol. 47, no. 12, pp. 2237–2241, Dec. 1999.
[4] Z.-W. Miao and Z.-C. Hao, "A wideband reflectarray antenna using substrate integrated coaxial true-time delay lines for QLink-pan applications," *IEEE Antennas Wireless Propag. Lett.*, vol. 16, pp. 2582–2585, 2017.
[5] J. A. Encinar, L. S. Datashvili, J. A. Zornoza, M. Arrebola, M. Sierra-Castaner, J. L. Besada-Sanmartin, H. Baier, and H. Legay, "Dual-polarization dual-coverage reflectarray for space applications," *IEEE Trans. Antennas Propag.*, vol. 54, no. 10, pp. 2827–2837, Oct. 2006.
[6] E. Martinez-de-Rioja, J. A. Encinar, M. Barba, R. Florencio, R. R. Boix, and V. Losada, "Dual polarized reflectarray transmit antenna for operation in Ku- and ka-bands with independent feeds," *IEEE Trans. Antennas Propag.*, vol. 65, no. 6, pp. 3241–3246, Jun. 2017.

[7] E. Carrasco, M. Barba, and J. A. Encinar, "X-band reflectarray antenna with switching-beam using PIN diodes and gathered elements," *IEEE Trans. Antennas Propag.*, vol. 60, no. 12, pp. 5700–5708, Dec. 2012.

[8] A. Yu, F. Yang, A. Z. Elsherbeni, J. Huang, and Y. Kim, "An offset-fed X-band reflectarray antenna using a modified element rotation technique," *IEEE Trans. Antennas Propag.*, vol. 60, no. 3, pp. 1619–1624, Mar. 2012.

[9] J. Yang, Y. Shen, L. Wang, H. Meng, W. Dou, and S. Hu, "2-D scannable 40-GHz folded reflectarray fed by SIW slot antenna in single-layered PCB," *IEEE Trans. Microw. Theory Techn.*, vol. 66, no. 6, pp. 3129–3135, Jun. 2018.

[10] K. H. Sayidmarie and M. E. Bialkowski, "Investigations into unit cells offering an increased phasing range for single-layer printed reflectarrays," *Microw. Opt. Technol. Lett.*, vol. 50, no. 4, pp. 1028–1032, Apr. 2008.

[11] L. Li, Q. Chen, Q. Yuan, K. Sawaya, T. Maruyama, T. Furuno, and S. Uebayashi, "Novel broadband planar reflectarray with parasitic dipoles for wireless communication applications," *IEEE Antennas Wireless Propag. Lett.*, vol. 8, pp. 881–885, 2009.

[12] Q.-Y. Chen, S.-W. Qu, X.-Q. Zhang, and M.-Y. Xia, "Low-profile wide-band reflectarray by novel elements with linear phase response," *IEEE Antennas Wireless Propag. Lett.*, vol. 11, pp. 1545–1547, 2012.

[13] Y. Li and L. Li, "Broadband microstrip beam deflector based on dual-resonance conformal loops array," *IEEE Trans. Antennas Propag.*, vol. 62, no. 6, pp. 3028–3034, Jun. 2014.

[14] M. R. Chaharmir, J. Shaker, and H. Legay, "Broadband design of a single layer large reflectarray using multi cross loop elements," *IEEE Trans. Antennas Propag.*, vol. 57, no. 10, pp. 3363–3366, Oct. 2009.

[15] E. Carrasco, J. S. Gomez-Diaz, M. Esquius-Morote, and J. R. Mosig, "Reflectarray elements in substrate integrated waveguides (SIW)," in *Proc. IEEE Int. Symp. Antennas Propag.*, Memphis, TN, USA, 2014, pp. 1–4.

[16] J. Zang, E. Carrasco, X. Wang, J. A. Encinar, A. Alvarez-Mclcon, and J. S. Gomez-Diaz, "SIW-based reflectarray antennas with sharp gain selectivity and large bandwidth," in *Proc. IEEE Int. Symp. Antennas Propag. USNC/URSI Nat. Radio Sci. Meeting*, Boston, MA, USA, Jul. 2018, pp. 1405–1406.

[17] E. Carrasco, J. A. Encinar, and M. Barba, "Bandwidth improvement in large reflectarrays by using true-time delay," *IEEE Trans. Antennas Propag.*, vol. 56, no. 8, pp. 2496–2503, Aug. 2008.

[18] I. Derafshi, N. Komjani, and M. Mohammadirad, "A single-layer broadband reflectarray antenna by using quasi-spiral phase delay line," *IEEE Antennas Wireless Propag. Lett.*, vol. 14, pp. 84–87, 2015.

[19] B. D. Nguyen, K. T. Pham, V.-S. Tran, L. Mai, and N. Yonemoto, "Reflectarray element using cut-ring patch coupled to delay line," *IEEE Antennas Wireless Propag. Lett.*, vol. 14, pp. 571–574, 2015.

[20] S. M. A. Momeni Hasan Abadi and N. Behdad, "Broadband true-time-delay circularly polarized reflectarray with linearly polarized feed," *IEEE Trans. Antennas Propag.*, vol. 64, no. 11, pp. 4891–4896, Nov. 2016.

[21] R. E. Munson, H. A. Haddad, and J. W. Hanlen, "Microstrip reflectarray for satellite communication and radar cross-section enhancement or reduction," U.S. Patent 4 684 952, Aug. 4, 1987.

[22] J. Huang, "Microstrip reflectarray," in *Proc. IEEE Int. Symp. Antennas Propag.*, London, ON, Canada, Jun. 1991, pp. 612–615.

[23] Y. Zhuang, K. L. Wu, C. Wu, and J. Litva, "Microstrip reflectarray: Full-wave analysis and design scheme," in *Proc. IEEE AP-S/URSI Symp.*, Ann Arbor, Michigan, Jun. 1993, pp. 1386–1389.

[24] C. Fan, W.-W. Choi, W. Yang, W. Che, and K.-W. Tam, "A low cross-polarization reflectarray antenna based on SIW slot antenna," *IEEE Antennas Wireless Propag. Lett.*, vol. 16, pp. 333–336, 2017.

[25] R. J. Cameron, C. M. Kudsia, and R. R. Mansour, *Microwave Filters for Communication Systems: Fundamentals, Design and Applications*. New York, NY, USA: Wiley, 2007.

[26] Y. He, G. Macchiarella, G. Wang, W. Wu, L. Sun, L. Wang, and R. Zhang, "A direct matrix synthesis for in-line filters with transmission zeros generated by frequency-variant couplings," *IEEE Trans. Microw. Theory Techn.*, vol. 66, no. 4, pp. 1780–1789, Apr. 2018.

[27] N. Lenin and P. H. Rao, "Evaluation of the reflected phase of a patch using waveguide simulator for reflectarray design," *Microw. Opt. Technol. Lett.*, vol. 45, no. 6, pp. 528–531, Jun. 2005.

[28] G. Matthaei, L. Young, and E. M. T. Jones, *Microwave Filters, Impedance-Matching Networks, and Coupling Structures*. Dedham, MA, USA: Artech House, 1980.

[29] ANSYS Inc. *ANSYS HFSS*. Accessed: 2020. [Online]. Available: http://www.ansys.com/Products/Electronics/ANSYS-HFSS

[30] J. R. Montejo-Garai, "Synthesis of filters with transmission zeros at real frequencies by means of trisections including source/load to resonator coupling," *Electron. Lett.*, vol. 36, no. 19, pp. 1629–1630, Sep. 2000.

[31] J. S. Hong and M. J. Lancaster, *Microstrip Filters for RF/Microwave Applications*. Hoboken, NJ, USA: Wiley, 2001.

[32] *Bay Area Circuits*. Accessed: 2019. [Online]. Available: https://store.bayareacircuits.com

[33] S. D. Targonski and D. M. Pozar, "Minimization of beam squint in microstrip reflectarrays using an offset feed," in *IEEE Antennas Propag. Soc. Int. Symposium. Dig.*, Baltimore, MD, USA, Jul. 1996, pp. 1326–1329.

JIAWEI ZANG (Member, IEEE) received the Ph.D. degree in electrical engineering from the Beijing Institute of Technology, Beijing, China, in 2019.

From September 2017 to November 2018, he was a Visiting Student with the Department of Electrical and Computer Engineering, University of California at Davis. His research interests include antennas, filters, and nonreciprocal components.

EDUARDO CARRASCO (Senior Member, IEEE) received the bachelor's degree in telecommunication engineering from the National Autonomous University of Mexico (UNAM), Mexico City, in 2000, and the Ph.D. degree in telecommunication engineering from the Technical University of Madrid (UPM), Madrid, Spain, in 2008.

From 1999 to 2001, he worked as a Broadcast Operations Systems Specialist with DIRECTV Latin America. In 2002, he received a Grant from the Vodafone Foundation to pursue a degree in telecommunications management at the School for Industrial Organization (EOI), Spain. From January to April 2008, he visited the Microwave Engineering Laboratory, University of Perugia, Italy, as a part of the Ph.D. research work. From June 2009 to June 2012, he was a Postdoctoral Researcher with the Electromagnetism and Circuits Theory Department, UPM, where he participated in various projects supported by the Spanish Government, the Mexican Council of Science and Technology (CONACYT), the European Union's Sixth and Seventh Framework (FP6 and FP7) Programs, and the European Space Agency (ESA). From 2012 to 2014, he worked as a Marie-Curie Fellow with the Adaptive Micronano Wave Systems Group, Swiss Federal Institute of Technology Lausanne (EPFL), Switzerland. He was with the Foundation for Research on Information Technologies in Society (IT'IS Foundation), Zürich, Switzerland, from January 2015 to September 2017, as an Electromagnetics (EM), a Dosimetry, and an Antenna Engineer. Since October 2017, he has been a member of the Information Processing and Telecommunications Center and an Assistant Professor with the Signals, Systems and Radiocommunications Department, UPM. His main research interests include the design of reconfigurable antenna arrays, including reflect and transmit arrays, from microwave to terahertz frequencies, EMF exposure, hyperthermia treatment planning, and other bioelectromagnetics topics.

XUETIAN WANG received the B.E. and Ph.D. degrees in electronic engineering from the Beijing Institute of Technology, Beijing, China, in 1986 and 2002, respectively.

He is currently a Full Professor with the School of Information and Electronics, Beijing Institute of Technology. His current research interests include antenna theory and applications, millimeter-wave imaging, EMC, and terahertz radar.

ALEJANDRO ALVAREZ-MELCON (Senior Member, IEEE) was born in Madrid, Spain, in 1965. He received the bachelor's degree in telecommunications engineering from the Technical University of Madrid (UPM), Madrid, in 1991, and the Ph.D. degree in electrical engineering from the Swiss Federal Institute of Technology Lausanne, Switzerland, in 1998.

In 1988, he joined the Signal, Systems and Radiocommunications Department, UPM, as a Research Student, where he was involved in the design, testing, and measurement of broad-band spiral antennas for electromagnetic measurements support (EMS) equipment. From 1991 to 1993, he was with the Radio Frequency Systems Division, European Space Agency (ESA/ESTEC), Noordwijk, The Netherlands, where he was involved in the development of analytical and numerical tools for the study of waveguide discontinuities, planar transmission lines, and microwave filters. From 1993 to 1995, he was with the Space Division, Industry Alcatel Espacio, Madrid, and the ESA, where he collaborated in several ESA/European Space Research and Technology Centre (ESTEC) contracts. From 1995 to 1999, he was with the Swiss Federal Institute of Technology, Ecole Polytechnique Federale de Lausanne (EPFL), Lausanne, Switzerland, where he was involved in the field of microstrip antennas and printed circuits for space applications. In 2000, he joined the Technical University of Cartagena, Spain, where he is currently developing his teaching and research activities. He was an Invited Professor with the Polytechnique Montr é al, Canada, from July 2010 to September 2010, and a Visiting Professor with the University of California at Davis, USA, from October 2017 to September 2018.

Dr. Alvarez-Melcon was a recipient of the Journee Internationales de Nice Sur les Antennes (JINA) Best Paper Award for the best contribution to the JINA 98 International Symposium on Antennas and the Colegio Oficial de Ingenieros de Telecomunicacion (COIT/AEIT) Award to the Best Ph.D. Dissertation in basic information and communication technologies.

JUAN SEBASTIAN GOMEZ-DIAZ (Senior Member, IEEE) was born in Ontur, Spain. He received the M.Sc. and Ph.D. degrees in electrical engineering from the Technical University of Cartagena, Cartagena, Spain, in 2006 and 2011, respectively.

During the development of the Ph.D. degree, he held visiting research positions at the École Polytechnique de Montréal, Canada, and the Fraunhofer Institute for High Frequency Physics and Radar Techniques, Germany. From October 2011 to March 2014, he was a Postdoctoral Fellow with the École Polytechnique Fédéral de Lausanne (EPFL), Switzerland. From May 2014 to August 2016, he continued his Postdoctoral work at the Metamaterials and Plasmonic Research Laboratory, The University of Texas at Austin. He is currently an Assistant Professor with the Electrical and Computer Engineering Department, University of California at Davis. His main research interests include multidisciplinary areas of electromagnetic wave propagation and radiation, metamaterials and metasurfaces, plasmonics, 2D materials, nonreciprocal and nonlinear phenomena, and other emerging topics on applied electromagnetics and nanotechnology.

Dr. Gomez-Diaz was a recipient of the NSF CAREER Award, the 2017 Leopold Felsen Award for Excellence in Electrodynamics, the Raj Mittra Award presented by the 2015 IEEE Antennas and Propagation Society, the Young Scientist Award of the 2015 URSI Atlantic RadioScience Conference, the FP7 Marie Curie Fellowship from the European Commision, in 2012, the Colegio Oficial de Ingenieros de Telecomunicación (COIT/AEIT) Award to the Best Spanish Ph.D. Thesis in basic information and communication technologies, in 2011, and the Best Ph.D. Thesis Award from the Technical University of Cartagena. He serves as a Reviewer for several journals on antennas, microwaves/terahertz, and physics.